

The effects of CO₂ database on a localized AquaCrop model construction based on the field experiment

fawen li (✉ lifawen@tju.edu.cn)

Tianjin university

chunya song

Tianjin university

hua li

Survey and Management Center of Hydrology and Water Resources, Tianjin

Research Article

Keywords: AquaCrop model, Winter wheat, CO₂, Evapotranspiration, Soil water content

Posted Date: August 10th, 2021

DOI: <https://doi.org/10.21203/rs.3.rs-747747/v1>

License:  This work is licensed under a Creative Commons Attribution 4.0 International License.

[Read Full License](#)

1 The effects of CO₂ database on a localized AquaCrop model
2 construction based on the field experiment

3 Fawen Li^{1*}, Chunya Song¹, Hua Li²

4 (1. State Key Laboratory of Hydraulic Engineering Simulation and Safety, Tianjin
5 University, Tianjin 300072, PR China; 2. Survey and Management Center of Hydrology
6 and Water Resources, Tianjin 300061, PR China)

7 The corresponding author's contact information:

8 Fawen Li, email: lifawen@tju.edu.cn

9 **Abstract:** To examine whether the use of default CO₂ database affected the simulation
10 results, this paper built the AquaCrop models of winter wheat based on the measured
11 CO₂ database and the default CO₂ database, respectively. The models were calibrated
12 with data (2017–2018) and validated with the data (2018-2019) in the North China Plain.
13 The residual coefficient method (CRM), root mean square error (RMSE), normalized
14 root mean square error (NRMSE) and determination coefficient (R^2) were used to test
15 the model performance. The results showed that the accuracy of simulation under the
16 two CO₂ database were both good. Compared with the default CO₂ database, the
17 simulation accuracy under the measured CO₂ database had higher accuracy. In order to
18 verify the model further, the simulated values of evapotranspiration, soil water content
19 and measured values were compared and analyzed. The results showed that there were
20 some errors between the measured evapotranspiration and the values of simulation in
21 the filling and waxing period of winter wheat. In general, the simulation values of

22 evapotranspiration were consistent with the measured value at different irrigation levels.
23 The simulated values of the soil water content at the three levels of irrigation were all
24 higher than the measured values, but the simulated results basically reflected the
25 dynamic changes of soil water content throughout the growth period. The model
26 adjustment value of WP*(the normalized water productivity) were a difference under
27 the two CO₂ databases, which is one of the reasons for the difference in the simulation
28 results. The results show that in the absence of measured CO₂ data, the default CO₂
29 database can be used, which has little influence on the model construction, and the
30 accuracy of the model constructed meets the actual demand. The research results can
31 provide a basis for the establishment of crop models in North China Plain.

32 **Keywords:** AquaCrop model; Winter wheat; CO₂; Evapotranspiration; Soil water
33 content

34

35

36

37 **1 Introduction**

38 The water on the earth is about 1.4 billion km³, however, the available water is less
39 than 45,000 km³ (about 0.003% of the total), and only 9,000 to 14,000 km³ (about 0.001%
40 of the total) suitable for human use. At present, about 1.5 billion people are facing a
41 shortage of fresh water in more than 80 countries around the world, of which 300
42 million people in 26 countries are living in a state of water shortage. It is estimated that
43 3 billion people in the world will be short of water, involving more than 40 countries
44 and regions by 2025. In the 21st century, water resource is becoming a precious and
45 scarce resource. The problem of water resource is not only a matter of resources, but a
46 major strategic issue that relates to the sustainable development of the country's
47 economy, society, and long-term security. China, the world's most populous developing
48 country, feeds 22% of the world's population with 7% of the world's land and 8% of its
49 fresh water. However, as the population continues to grow, the climate is arid, pollution
50 continues to worsen, and water and arable land resources continue to decrease, China
51 will face huge pressures and challenges in terms of water resources and food security
52 (Zhang et al.2005). The North China Plain covers an area of 0.44×10^6 km² and has a
53 population of over 200 million. It is one of the most productive and intensive
54 agricultural areas in China (Iqbal et al. 2014). The main crops are wheat and corn. The
55 wheat and corn production account for 20% of the country's total output, of which wheat
56 accounts for 11% and corn accounts for 9%. Due to the growth cycle of winter wheat
57 from October to June of the second year, it is the time when water is supplied the most

58 insufficient in North China, a large amount of groundwater has been over-exploited for
59 irrigation. There is a more prominent contradiction between water resources and food
60 security issues in North China. To solve water resources and food security issues, it is
61 necessary to build a water-driven crop growth model to simulate and formulate a
62 reasonable future adjustment schemes of food crops pattern (Xia et al. 2004).

63 At present, a series of crop growth models have been developed, such as CERES-
64 Maize (Kisekka et al. 2016), WOFOST (Diepen et al. 2007), CropSyst (Stockle et al.
65 2003), DSSAT-CSM (Jones et al. 2003), and the Hybrid Maize model (Yang et al. 2004).
66 However, due to the complexity of these models and the large number of input
67 parameters, it is difficult to use such models for popularization and application (Malik
68 et al. 2017). The Food and Agriculture Organization (FAO) of the United Nations
69 developed the AquaCrop model in 2009. Compared with above models, AquaCrop is
70 user-friendly and practitioner-oriented software (Ahmadi et al. 2015). The AquaCrop
71 model has been extensively tested and applied in different regions (Raes et al. 2009;
72 Bird et al. 2016; Li et al. 2019). The main problem of the AquaCrop model is the
73 applicability. Hsiao et al. (2009) concluded that the applicability of the AquaCrop
74 model should be further verified for different soil properties, crop characteristics and
75 climatic conditions around the world. Yin et al. (2013) studied the applicability of the
76 AquaCrop model in semi-arid regions and applied the AquaCrop model to the
77 management of deficient irrigation of spring wheat, and got irrigation regimes in
78 different years. Iqbal et al. (2014) studied the applicability of the AquaCrop model in

79 the North China Plain and simulated winter wheat biomass, yield, actual
80 evapotranspiration and total soil water content (0-120 cm). Mhizhat et al. (2014)
81 calibrated the AquaCrop model by using measured corn data, and simulated yield
82 through an optimized program. Sylaios (2016) used nine years of climate data from
83 Northern Greece and a locally calibrated AquaCrop model to test an efficient model-
84 based procedure for computing seasonal sub-optimal irrigation schedules. Sandhu and
85 Irmak (2019) evaluated the AquaCrop model relative to maize growth, yield, and water
86 use parameters/variables under different water stress conditions over six years (2005-
87 2010) in Nebraska, USA. Li et al. (2019) studied the applicability of the model in North
88 China Plain and applied the AquaCrop model to optimize irrigation strategies.

89 The above researchers run the AquaCrop model with the default CO₂ database
90 (MaunaLoa.CO2 file). When the measured CO₂ database are missing, AquaCrop will
91 automatically apply the default CO₂ database. Actually, the CO₂ concentration had
92 effects on crop growth (Xiao et al. 2005; Meng et al. 2015; Ma et al. 2005; Li et al.
93 2020). In this study, a local Aquacrop model was established to simulate the biomass
94 and yield of winter wheat based on the measured and default CO₂ database, and analyze
95 how much influence the default database can have on the simulation results of the
96 model in North China Plain.

97 **2 Materials and methods**

98 2.1 Study Area

99 The North China Plain (NCP) is one of the most productive agricultural regions in
100 China. The 70% of the water used in the wheat-growing seasons comes from
101 groundwater pumped from wells with a depth of over 40 m, causing a rapid decline in
102 the groundwater table in the NCP (Yuan et al. 2013). With climate change in the NCP,
103 the contradiction between water resources and agricultural water demand will be further
104 intensified (Falloon et al. 2010).

105 The study area is located in the NCP and its coordinate is 37°30'~38°18' N and
106 114°19'~116°30' E, with an average altitude of 42 m (Fig. 1). The annual rainfall is
107 455.8mm, which is concentrated in June to September, and mean annual evaporation is
108 approximately 1000~1200 mm, which is characteristic of a semi-arid sub-humid
109 monsoon climate with the average annual temperature of 13.3°C, the average number
110 of sunshine hours of 2397.2 h and the annual frost-free period of 236 d.

111 The selected cultivar of winter wheat was Guan-35, the seeding rate was 187.5
112 kg·ha⁻¹. The sowing time was in mid to late October of each year, and the harvest time
113 was in early June of the next year. The winter wheat planting time for the 2017-2018
114 season and 2018-2019 season were October 28 and October 17, respectively. There
115 were nine test plots, each with an area of 8 m×15 m. The irrigation mode was border
116 irrigation, which was carried out in the wintering period, jointing period and grouting
117 period respectively. Before sowing, a compound fertilizer was applied as the base

118 fertilizer, and the fertilizer amount was 750kg/hm². The tillage mode was rotary tillage.
119 The irrigation schedule of winter wheat for 2017-2019 was shown in Table 1. T1 is 100%
120 of the local irrigation level, T2 is 80% of the local irrigation level, and T3 is 60% of the
121 local irrigation level in Table1.

122 2.2 Description of AquaCrop Model

123 The principle of AquaCrop model was the crop yield-water effect relationship
124 proposed by Doorenbos and Kassam (1979), which was expressed as follows:

$$125 \quad \frac{Y_m - Y_a}{Y_m} = K_y \left(\frac{ET_m - ET_a}{ET_m} \right) \quad (1)$$

126 Where Y_m and Y_a are the maximum output (kg · m⁻²) and actual output (kg·m⁻²),
127 respectively; ET_m is the maximum evapotranspiration (mm) and ET_a is actual
128 evapotranspiration (mm); K_y is the crop yield response factor (dimensionless).

129 In AquaCrop, ET is decomposed into E and Tr, which can avoid the interference of
130 soil evaporation on crop yield, especially when the canopy coverage is reached the
131 maximum (CCmax). The core formula of AquaCrop are as follows (Steduto et al. 2009):

$$132 \quad B = WP^* \cdot \sum \frac{Tr}{ET_0} \quad (2)$$

$$133 \quad Y = B \cdot HI \quad (3)$$

134 Where WP^* is the normalized crop water productivity (g · m⁻²), and its value varies
135 with the annual average CO₂ concentration and the difference in crop species; B is the
136 cumulative aboveground biomass production (g · m⁻²); Tr is the daily crop transpiration

137 (mm • day⁻¹); ET_0 is the daily reference evapotranspiration (mm • day⁻¹); Y is the yield
 138 production (g • m⁻²); and HI is the harvest index (%).

139 In AquaCrop model, the aboveground biomass is simulated by the normalized water
 140 productivity (WP*) (Eq.2). The WP* is normalized for atmospheric CO₂ concentration,
 141 using the annual mean CO₂ concentration measured at Mauna Loa Observatory, Hawaii,
 142 for each of the years. The year 2000, with its mean CO₂ concentration of 369.41 ppm,
 143 is chosen as the reference year for CO₂. AquaCrop will adjust WP* when running a
 144 simulation for a year at which the atmospheric CO₂ concentration differs from its
 145 reference value (369.41 ppm). The adjustment is obtained by multiplying WP* with the
 146 correction coefficient f_{CO_2} (Vanuytrecht et al., 2011). The coefficient considers the
 147 difference between the reference value and the atmospheric composition for that year:

$$WP_{adj}^* = f_{CO_2} WP^* \quad (4)$$

$$f_{CO_2} = \frac{([CO_2]_i/[CO_2]_o)}{1 + ([CO_2]_i - [CO_2]_o)[(1 - w)b_{sted} + w(f_{sink}b_{sted} + (1 - f_{sink})b_{FACE})]} \quad (5)$$

$$0 \leq w = \left(1 - \frac{550 - [CO_2]_i}{550 - [CO_2]_o}\right) \leq 1 \quad (6)$$

148 where WP_{adj}^* is WP adjusted for CO₂; f_{CO_2} is correction coefficient for CO₂; $[CO_2]_o$
 149 is reference atmospheric CO₂ concentration (369.41 ppm); $[CO_2]_i$ is actual atmospheric
 150 CO₂ concentration for year i (ppm); the value of b_{sted} is 0.000138 (Steduto et al., 2007);
 151 b_{FACE} is 0.001165 (derived from FACE experiments); w is weighing factor, the
 152 threshold of 550 ppm is selected as the representing value for the elevated CO₂

153 maintained in the FACE experiments; f_{sink} is crop sink strength coefficient. The value
154 of f_{sink} is taken as zero in this study (based on an analysis of crop responses in FACE
155 environments by Vanuytrecht et al., 2011).

156 2.3 Construction of the AquaCrop model

157 The most important parameters of crops included initial canopy coverage, threshold
158 for extreme growth temperature, maximum effective root depth, and planting density.
159 The soil parameters in the model included: saturated moisture content, permanent
160 wilting point content, and initial value of field capacity etc., which need to be set
161 according to the soil characteristics of the experimental fields.

162 *Input model parameters*

163 The soil texture in the experimental fields is loam. The depth of soil in the
164 experimental fields is 0~120cm, which is divided into 6 layers with each layer thickness
165 of 20 cm. The soil characteristics of each layer were shown in Table 2.

166 During the two-season winter wheat growth period of 2017-2019, soil samples of 0
167 ~ 60cm deep were collected every 5~10 days, and soil water content (SWC) was
168 measured by sampling every 10cm. The SWC was measured before and after irrigation
169 in the key growth stages of winter wheat (seeding period, overwintering period, jointing
170 period, filling period and maturity period).

171 The meteorological data came from the data monitored by the automatic
172 meteorological station installed in the experimental fields, of which data were recorded

173 at intervals of 30min, including temperature, relative humidity, wind speed at 2m
174 altitude, duration of sunshine, atmospheric pressure, rainfall, heat flux, net radiation,
175 etc. Reference evapotranspiration (ET_0) can be estimated by Penman-Monteith
176 equation, and the ET_0 calculation software recommended by the Land and Water
177 Division of FAO was applied to calculate the reference crop evapotranspiration.

$$178 \quad ET_0 = \frac{0.408\Delta(R_n - G) + \frac{900}{T+273}U_2(e_s - e_a)}{\Delta + \gamma(1 + 0.34U_2)} \quad (7)$$

179 Where R_n is the net radiation on the crop surface ($MJ \cdot m^{-2} \cdot d^{-1}$); G is the soil heat
180 flux ($MJ \cdot m^{-2} \cdot d^{-1}$), T is the average temperature ($^{\circ}C$), U_2 is the average at a height of 2
181 m Wind speed ($m \cdot s^{-1}$), e_s is the saturated water pressure (kPa), e_a is the actual water
182 pressure (kPa), Δ is the slope of the saturated water vapor pressure and temperature
183 curve ($kPa \cdot ^{\circ}C^{-1}$), γ is the dry and wet surface constant ($kPa \cdot ^{\circ}C^{-1}$).

184 An equipment, Agilent 5890 SERIES II gas chromatograph, can be applied to
185 measure the CO_2 concentration in the experimental fields. The conditions for analyzing
186 and detecting atmospheric CO_2 with 5890 SERIES II gas chromatograph: silica gel
187 column (aged at $150^{\circ}C$ for 24h before measurement), injection temperature is $130^{\circ}C$,
188 oven temperature is $120^{\circ}C$, detector temperature is $150^{\circ}C$. The carrier gas of TCD
189 (thermal conductivity detection) is high purity N_2 (mol/mol, $\geq 99.999\%$) which flow
190 velocity is 40ml/min; the sample volume of the gas is 1.0 ml, and the retention time of
191 CO_2 peak area on the chromatogram is 1.5min.

192 Determination of CO_2 concentration: the CO_2 concentration of atmospheric samples
193 were determined within 2 days by using the gas chromatograph. When the sample of

194 CO₂ was collected, the atmospheric temperature was recorded at the same time each
195 time. The gas samples were collected by using professional gas pump equipment
196 starting from 10 o'clock in the morning for a total of four times at each 20 minutes. The
197 gas sample was collected at each 5~7d, and the sample gas was added 2~3 times in case
198 of irrigation, fertilization, etc.

199 CO₂ concentration detection method: a standard gas with known CO₂ concentration
200 were injected into the gas chromatograph to obtain the stable peak area values of the
201 standard gas (the error of two consecutive peak areas is within 0.1%). The CO₂
202 concentration of the sample gas were detected based on the peak area and the known
203 CO₂ concentration of the standard gas.

204 The change curve of atmospheric CO₂ concentration in the two seasons of winter
205 wheat (2017-2018, 2018-2019 season) was shown (Fig.2). The two average
206 atmospheric CO₂ concentration during the growth period of winter wheat was
207 462.6ppm and 478.0 ppm, respectively. Based on the measured CO₂ concentrations, a
208 CO₂ database suitable for the local climatic conditions in the experimental fields was
209 established instead of the default CO₂ database (Maunaloa.CO₂) provided by the model
210 itself.

211 The AquaCrop provided physiological parameters for 14 crops including cotton,
212 corn, wheat, potato, rice etc. Some parameters were conservative parameters (Table 3).
213 Other winter wheat parameters need to be calibrated by AquaCrop model.

214 |Model evaluation

215 The performance of the model was evaluated using the following indicators: the
216 root mean square error (RMSE), residual coefficient method (CRM), normalized root
217 mean square error (NRMSE) and determination coefficient (R^2).

218
$$RMSE = \sqrt{\frac{\sum_{i=1}^n (P_i - O_i)^2}{n}} \quad (8)$$

219
$$CRM = \frac{\sum_{i=1}^n O_i - \sum_{i=1}^n P_i}{\sum_{i=1}^n O_i} \times 100\% \quad (9)$$

220
$$NRMSE = \frac{100}{\bar{O}} \sqrt{\frac{\sum_{i=1}^n (P_i - O_i)^2}{n}} \quad (10)$$

221
$$R^2 = \left[\frac{\sum_{i=1}^n (O_i - \bar{O})(P_i - \bar{P})}{\sqrt{\sum_{i=1}^n (O_i - \bar{O})^2} \sqrt{\sum_{i=1}^n (P_i - \bar{P})^2}} \right]^2 \quad (11)$$

222 Where n is the total number of observations of the sample, O_i and P_i are the
223 observations and simulation values, respectively. \bar{O} and \bar{P} are the average of all
224 observation and simulation values, respectively. RMSE indicates the deviation between
225 the observed value and the simulation value. The smaller the value is, the higher the
226 accuracy of the model indicates. The smaller CRM value of the coefficient is, the better
227 the simulation effect shows. When the value of NRMSE is less than 10%, the simulation
228 effect is high. A value between 10% and 20% indicates that the simulation result is good,
229 while between 20% and 30% indicates that the simulation effect is average. The value
230 of R^2 ranges from 0 to 1, with values close to 1 indicating a good agreement, and
231 typically values greater than 0.5 are considered acceptable in watershed simulations
232 (Moriasi et al., 2007).

233 **3 Results and discussion**

234 3.1 Analysis of biomass and yield simulation results under two CO₂ databases

235 In order to analyze the differences in simulation results of using the various CO₂
236 databases, the default CO₂ database (Maunaloa.CO₂) and the measured CO₂ database
237 were used to simulate. The results of the winter wheat biomass under different CO₂
238 databases were shown in Tables 4 and 6, respectively, and the results of the yield were
239 shown in Tables 5 and 7 respectively.

240 The CRM values range of the winter wheat biomass simulation values in 2017-2018
241 season were -1.193%~1.844% under the default CO₂ database (Maunaloa.CO₂) in Table
242 4, and the values (2018-2019 season) were -0.676%~0.932%. The values of RMSE
243 ranged from 0.037~0.257 t·ha⁻¹ in 2017-2018 season, and the values (2018-2019 season)
244 were 0.130~0.299 t·ha⁻¹. The values of NRMSE (2017-2018 season) were
245 0.298%~1.948%, and the values (2018-2019 season) were 0.864% to 2.076%. The
246 absolute CRM values were less than 2.0%, the values of RMSE were less than 0.300
247 t·ha⁻¹, and the NRMSE values were less than 2.5%. Overall, the errors between the
248 simulated and measured values of winter wheat biomass were small.

249 The range of CRM winter wheat (2017-2018 season) yield simulation values was -
250 0.559% to -0.073%, and the range of CRM (2018-2019 season) was -0.059% to 3.049%
251 under the default CO₂ database (Maunaloa.CO₂) in Table 5. The value of RMSE for
252 winter wheat (2017-2018 season) was between 0.025 t·ha⁻¹ and 0.142 t·ha⁻¹, and the
253 value (2018-2019 season) was in the range of 0.045~0.238 t·ha⁻¹. The value of NRMSE

254 (2017-2018 season) ranged from 0.447% to 2.327%, and the value (2018-2019 season)
255 ranged from 0.741% to 3.327%. The absolute CRM values were all less than 3.5%, the
256 RMSE values were less than $0.25 \text{ t}\cdot\text{ha}^{-1}$, and the NRMSE values were less than 3.5%,
257 which indicated that the precise of yield simulation were good. Overall, the errors
258 between the simulated and measured values of winter wheat yield were small.

259 The CRM range of winter wheat (2017-2018 season) biomass simulation values
260 was $-0.727\% \sim 1.151\%$, and the CRM range (2018-2019 season) was -0.273% to 0.100%
261 under the measured CO_2 database in Table 6. The values of RMSE ranged from
262 $0.057 \sim 0.204 \text{ t}\cdot\text{ha}^{-1}$, and the range (2018-2019 season) was $0.011 \sim 0.114 \text{ t}\cdot\text{ha}^{-1}$. The
263 values of NRMSE (2017-2018 season) ranged from 0.456% to 1.544%, and the values
264 (2018-2019 season) ranged from 0.084% to 0.793%. The absolute CRM values were
265 all less than 1.5%, RMSE values were less than $0.25 \text{ t}\cdot\text{ha}^{-1}$, and NRMSE values were
266 less than 2.0%, which indicated that the precise of biomass simulation was high.

267 The CRM range of winter wheat (2017-2018 season) yield simulation values was -
268 $1.204\% \sim -0.307\%$, and the range of the CRM (2018-2019 season) was $-1.055\% \sim -0.369\%$
269 under the measured CO_2 database in Table 7. The values of the RMSE ranged from
270 $0.050 \sim 0.078 \text{ t}\cdot\text{ha}^{-1}$ (2017-2018 season), and the range (2018-2019 season) was
271 $0.048 \sim 0.130 \text{ t}\cdot\text{ha}^{-1}$. The values of the NRMSE (2017-2018 season) ranged from
272 $0.843\% \sim 1.304\%$, and the range (2018-2019 season) was $0.679\% \sim 1.932\%$. The absolute
273 CRM values were all less than 1.5%, the RMSE values were less than $0.15 \text{ t}\cdot\text{ha}^{-1}$, and

274 the NRMSE values were less than 2.0%, which indicated that the precise of yield
275 simulation was high.

276 As can be seen from Fig.3 and Fig.4, the R^2 of biomass under different CO_2
277 databases for different irrigation levels of winter wheat were 0.992 and 0.967,
278 respectively. And the R^2 of the yield were 0.974 and 0.857, respectively. The accuracy
279 of the biomass and yield simulation under the default and measured CO_2 database were
280 both good. Compared with the default CO_2 database, the simulation accuracy of winter
281 wheat yield and biomass under the measured CO_2 database was higher. So, the
282 measured CO_2 database can improve the model simulation accuracy.

283 The water use efficiency of winter wheat in the 2018-2019 season under the
284 measured CO_2 database, were 1.63kg/m³, 1.72 kg/m³and 1.56 kg/m³, respectively,
285 under the three irrigation levels. The water use efficiency under the default CO_2
286 database were 1.66 kg/m³, 1.71 kg/m³ and 1.54 kg/m³, respectively. The water use
287 efficiency under the two CO_2 databases is the highest when the irrigation level is T2,
288 which is consistent with the research conclusion (Xing et al., 2016).

289 *Impact analysis of parameters under different CO_2 databases*

290 The calibration parameters of the AquaCrop under two different CO_2 databases
291 were shown in Table 8. The calibration parameters included the length building up HI,
292 the maximum root depth, water productivity and crop growth temperature. According
293 to formulas 4-6, the values in parentheses are the adjusted values of WP*. When the

294 default CO₂ database was used in the model, there was a little influence on the
295 calibration parameters of the model.

296 **4 Validation of the AquaCrop model under the measured CO₂ database**

297 4.1 Validation analysis of field evapotranspiration

298 The ET_a (actual evapotranspiration), called measured evapotranspiration, can be
299 calculated according to the water balance method by using the data of rainfall and soil
300 water content. The water balance equation is as follows:

$$301 \quad ET_a = W_0 - W_t + P + I + K - R - D \quad (12)$$

302 Where ET_a is the crop evapotranspiration (mm); W_0 and W_t are the soil water storage
303 at the beginning and the end of the calculation period (mm); P is the precipitation (mm);
304 I is the amount of irrigation water (mm); K is the amount of groundwater recharge to
305 the upper layer, because the groundwater is buried deep in the study area, the amount
306 of groundwater recharge can be ignored (mm); R is the surface runoff (mm); D is the
307 deep leakage (mm). Because the amount of rainfall (or irrigation) is relatively small
308 and the land is relatively flat, surface runoff and deep leakage can be ignored.

309 It can be seen from Fig.5 that the change process of measured and simulated
310 evapotranspiration was consistent under different irrigation levels. The field
311 evapotranspiration was close to the measured value in the seedling, overwintering and
312 mature period. During the filling and waxing period of winter wheat, due to the
313 combined effect of rainfall and irrigation, there were some errors between the measured

314 values and the values of simulation. In general, the simulation values of field
315 evapotranspiration were consistent with the measured values of winter wheat (2018-
316 2019 season) under different irrigation levels.

317 The evapotranspiration of winter wheat was dominated by field soil evaporation
318 before and after seedling stage. The main reason was that the crop plants were small
319 and the bare soil was dominant in the field. So, the transpiration of the crop was smaller
320 than the soil evaporation. With the development of seedlings and the decrease of air
321 temperature, the evaporation capacity of field soil weakened. Field evapotranspiration,
322 soil evaporation and crop transpiration of winter wheat in overwintering period were
323 very small. When winter wheat was in the jointing stage, the plants grew and developed
324 rapidly as the temperature raised and the canopy of winter wheat expanded rapidly, too.
325 The transpiration of crops started to increase while the evaporation of soil started to
326 decrease. The transpiration of winter wheat gradually reached the maximum value from
327 the filling stage to the waxing stage. The field evapotranspiration and crop transpiration
328 began to decrease, concurrently, the soil evaporation began to increase at the mature
329 period of winter wheat.

330 4.2 Validation analysis of soil water content

331 The main factors affecting soil water storage were precipitation, ambient
332 temperature, field irrigation, and crop water consumption during the growth and
333 development of winter wheat. AquaCrop model is a water-driven model, so the crop

334 water consumption during the crop growth period determined the simulation precision
335 of crop biomass and yield. And the crop water consumption was mainly provided by
336 soil water content. Therefore, the performance of the AquaCrop model was determined
337 by the dynamic change of soil water content (Ahmadi et al. 2015). The process of soil
338 water content change (within the effective root depth of 0-140cm) in the test plots
339 during the growth period of winter wheat in 2018-2019 season were shown in Figure 6.

340 The errors between the simulated and the measured values of soil water content at
341 the irrigation amount (T1) and (T3) were large, while the errors under appropriate
342 irrigation amount (T2) was small in Figure 6. The reason might be that the smaller
343 irrigation amount (T3) had more severe effect on the growth of winter wheat by water
344 stress, which led to an increase demand for soil moisture during the growth of winter
345 wheat, resulting in a large deviation between the actual measured soil water content and
346 the simulated value. The larger irrigation amount (T1) may lead to deep leakage of soil
347 water, resulting in a large deviation between the simulated value and the measured value.
348 In addition, the simulation accuracy of the larger irrigation amount (T1) was higher
349 than that of the lower irrigation amount (T3). The reason might be that when the soil
350 was replenished with a large amount of irrigation, the soil can store redundant water to
351 meet the growth of the crop. When the amount of irrigation was small, soil moisture
352 cannot be replenished, and the impact of water stress on crop growth was increasing.
353 The simulated values of the AquaCrop model for soil water content at the three levels
354 of irrigation were all higher than the measured values. The deviation of the simulation

355 results might be caused by the differences of the soil structure and texture in the test
356 plots. At the same time, the failure of the AquaCrop model to take into account the
357 variability of soil texture and structure in the soil module was also the reason for the
358 deviation of the simulated values from the actual measured values. Overall, the
359 simulated values for soil water storage were larger than the measured values, but the
360 simulated results largely reflected the dynamic changes in soil water content throughout
361 the growth period of winter wheat.

362 **5 Conclusions**

363 (1) The AquaCrop model has been proven to simulate the biomass and yield of
364 winter wheat with good accuracy in North China Plain. However, the default CO₂
365 database was adopted in the simulation, which may affect the simulation results. To
366 examine whether the use of default CO₂ database affected the simulation results, this
367 paper built the AquaCrop models based on the measured CO₂ database and the default
368 CO₂ database, respectively. The results showed that the accuracy of the biomass and
369 yield simulation under the default and measured CO₂ database were all good, but the
370 latter has higher simulation accuracy.

371 (2) The difference between crop transpiration and soil evaporation under the two
372 CO₂ databases was not obvious, and the measured value was close to the field
373 evapotranspiration in the seedling, overwintering and mature period. During the filling
374 and waxing period of winter wheat, there were some errors between the measured

375 values of field evapotranspiration and the values of simulation. In general, the
376 simulation values of field evapotranspiration were consistent with the measured values
377 of winter wheat at different irrigation levels.

378 (3) The simulated values of the AquaCrop model for soil water content at the three
379 levels of irrigation were all higher than the measured values. The errors between the
380 simulated and the measured values of soil water content at the irrigation amount (T1)
381 and (T3) were larger than that of the irrigation amount (T2). Overall, the simulated
382 values for soil water storage were larger than the measured values, but the simulated
383 results largely reflected the dynamic changes in soil water content throughout the
384 growth period of winter wheat.

385 **Declarations**

386 **Data Availability**

387 The datasets used during the current study are available from the corresponding
388 author on reasonable request.

389 **Funding**

390 The authors would like to acknowledge the financial support for this work provided
391 by the National Natural Science Foundation of China (Grant no.51879181) and Global
392 Environment Facility Water Resources and Water Environment Management
393 Promotion (Mainstreaming) Project (P145897).

394 **Author information**

395 **Affiliations**

396 State Key Laboratory of Hydraulic Engineering Simulation and Safety, Tianjin
397 University, Tianjin 300072, PR China

398 Fawen Li, Chunya Song

399 Survey and Management Center of Hydrology and Water Resources, Tianjin 300061,
400 PR China

401 Hua Li

402 **Contributions**

403 All authors were involved in the production and writing of the manuscript.
404 Methodology, F.L. and C.S.; Formal Analysis, F.L. and C.S.; Data Curation, H.L.;
405 Review & Editing, F.L. and C.S.; All authors have read and agreed to the published
406 version of the manuscript.

407 **Corresponding author**

408 Correspondence to Fawen Li.

409 **Compliance with Ethical Standards**

410 Conflicts of interest/Competing interests

411 The authors declare that they have no competing interests.

412 Consent to Participate

413 The authors declare that they consent to participate.

414 Consent for Publication

415 The authors declare that they consent to publish.

416 **References**

- 417 Ahmadi S. H., Mosallaeepour E. (2015) Modeling maize yield and soil water content
418 with AquaCrop under full and deficit irrigation managements. *Water Resources*
419 *Management* 29(8):1-17.
- 420 Bird DN, Benabdallah S, Gouda N, Hummel F, Koeberl J, Jeunesse IL, Meyer S,
421 Pretenthaler F, Soddu A, Susanne WG. (2016) Modelling climate change impacts
422 on and adaptation strategies for agriculture in Sardinia and Tunisia using
423 AquaCrop and value-at-risk. *Science of the Total Environment* 543:1019-1027.
- 424 Diepen CV, Wolf J, Keulen HV, Rappoldt C (2007) WOFOST: a simulation model of
425 crop production. *Soil Use Management* 5(1):16–24.
- 426 Fu ZQ, Cai YL, Yang YX, Dai LF. (2001) Correlation analysis of China's food security
427 and arable land resource changes. *Journal of Natural Resources* (04):313-319.
- 428 Fu C, Li SS, Li J, Wang YC, Lu YS, Xu WZ, Wei S. (2012) Calibration and verification
429 of the AquaCrop crop model in the spring wheat area of the Songnen Plain. *Journal*
430 *of Irrigation and Drainage* 31(05): 99-102.
- 431 Falloon P, Betts R. (2010) Climate impacts on European agriculture and water
432 management in the context of adaptation and mitigation: the importance of an
433 integrated approach. *Science of the Total Environment* 408 (23), 5667–5687.

- 434 Hsiao TC, Heng L, Steduto R-LB, Raes D, Fereres E. (2009) AquaCrop-the FAO crop
435 model to simulate yield response to water: III. Parameterization and testing for
436 maize. *Agronomy Journal* 101(3):448-459.
- 437 Iqbal M A, Shen Y J, Stricevic R, Pei H W, Sun H Y, Amiri E, Penas A, Rio S D. (2014)
438 Evaluation of the FAO AquaCrop model for winter wheat on the North China Plain
439 under deficit irrigation from field experiment to regional yield simulation.
440 *Agricultural Water Management* 135:61-72.
- 441 Jones JW, Hoogenboom G, Porter CH, Boote KJ, Batchelor WD, Hunt LA (2003) Dssat
442 cropping system model. *European Journal of Agronomy* 18(3):235–265.
- 443 Kang SZ. (2014) Water security and food security. *Chinese Journal of Eco-Agriculture*,
444 22(08): 880-885.
- 445 Kisekka I, Aguilar JP, Rogers DH, Holman J, Brien DM, Klocke N. (2016) Assessing
446 deficit irrigation strategies for corn using simulation. *Transactions of the Asae*
447 *American Society of Agricultural Engineers* 59(1):303–317.
- 448 Li FW, Liu Y, Yan WH, Zhao Y, Jiang RG. (2020) Effects of future climate change on
449 summer maize growth in Shijin Irrigation District. *Theoretical and Applied*
450 *Climatology* 139(1-2):33-44.
- 451 Li FW, Yu D, Zhao Y. (2019) Irrigation Scheduling Optimization for Cotton Based on
452 the AquaCrop Model. *Water Resources Management* 33(1):33-55.

453 Ma HL, Zhu JG, Xie ZB, Liu G, Zhang YL, Zeng Q. (2005) Effects of Open-Air CO₂
454 Concentration on Growth and N Uptake of Winter Wheat. *Acta Agronomica Sinica*
455 (12):1634-1639.

456 Malik A, Shakir AS, Ajmal M, Khan MJ, Khan TA. (2017) Assessment of AquaCrop
457 Model in Simulating Sugar Beet Canopy Cover, Biomass and Root Yield under
458 Different Irrigation and Field Management Practices in Semi-Arid Regions of
459 Pakistan. *Water Resources Management* 31(13):4275-4292.

460 Meng FC, Zhang JH, Hao C, Zhou ZM, Li H, Liu D, Wang K, Zhang H. (2015) Effects
461 of CO₂ Concentration Increase and Different Irrigation Amounts on
462 Photosynthetic Characteristics and Yield of Northeast Corn. *Acta Ecologica Sinica*
463 35(07):2126-2135.

464 Mhizha T, Geerts S, Vanuytrecht E, Makarau A, Rase D. (2014) Use of the FAO
465 AquaCrop model in developing sowing guidelines for rain fed maize in Zimbabwe.
466 *Water SA* 40(2):233-243.

467 Moriasi D N, Arnold J G, Liew M W V, Bingner R L, Harmel R D, and Veith T L,
468 (2007). Model evaluation guidelines for systematic quantification of accuracy in
469 watershed simulations. *Transactions of The ASABE* 50, 885–900.

470 Raes D, Steduto P, Hsiao T C, et al. (2009) AquaCrop-the FAO crop model to simulate
471 yield response to water: II. Concepts and Underlying Principles. *Agronomy*
472 *Journal* 101(3):438-447.

473 Sandhu R, Irmak S. (2019) Performance of AquaCrop model in simulating maize
474 growth, yield, and evapotranspiration under rainfed, limited and full irrigation.
475 *Agricultural Water Management*, 223:105687.

476 Steduto P, Hsiao T C, Dirk R, et al. (2009) AquaCrop-the FAO crop model to simulate
477 yield response to water: I. Concepts and Underlying Principles. *Agronomy Journal*
478 101(3):426-437.

479 Stockle CO, Donatelli M, Nelson R. (2003) CropSyst a cropping systems simulation
480 model. *European Journal of Agronomy* 18:289–307.

481 Vanuytrecht E, Raes and Willems. 2011. Considering sink strength to model crop
482 production under elevated atmospheric CO₂. *Agricultural and Forest Meteorology*
483 151: 1753-1762.

484 Xia J, Liu MY, Jia SF. (2004) Thinking and research on water resources and water
485 security in North China. *Journal of Natural Resources* 19 (5):550-560.

486 Xiao GJ, Liu WX, Xu Q, Sun ZJ, Wang J. (2005) Effects of temperature increase and
487 elevated CO₂ concentration, with supplemental irrigation, on the yield of rain-fed
488 spring wheat in a semiarid region of China. *Agricultural Water Management*
489 3(74):243-255.

490 Xing HM, Xu XG, Feng HK, Li ZH, Yang FQ, Yang GJ, He P, Chen ZX. (2016) Water
491 use efficiency of winter wheat in Beijing area based on AquaCrop model. *Chinese*
492 *Agricultural Sciences* 49(23): 4507-4519.

493 Yang HS, Dobermann A, Lindquist JL, Walters DT, Arkebauer TJ, Cassman KG. (2004)
494 Hybrid-maize- a maize simulation model that combines two crop modeling
495 approaches. *Field Crop Research* 87:131–154.

496 Yin HX. (2013) Application of AquaCrop model in the management of spring wheat
497 irrigated in semi-arid areas. Lanzhou: Northwest Normal University.

498 Yuan ZJ, Shen YJ. (2013) Estimation of agricultural water consumption from
499 meteorological and yield data: a case study of Hebei, North China. *Plos One* 8,
500 e58685.

501 Zhang LP, Xia J, Hu ZF.(2009) Analysis of China's water resources status and water
502 security issues. *Resources and Environment in the Yangtze River Basin* 18(02):
503 116-120.

504 Zhang X, Chen S, Liu M, Pei D, Sun H. (2005) Improved water use efficiency
505 associated with cultivars and agronomic management in the north China plain.
506 *Agronomy Journal* 97, 783–790.

507

508

509

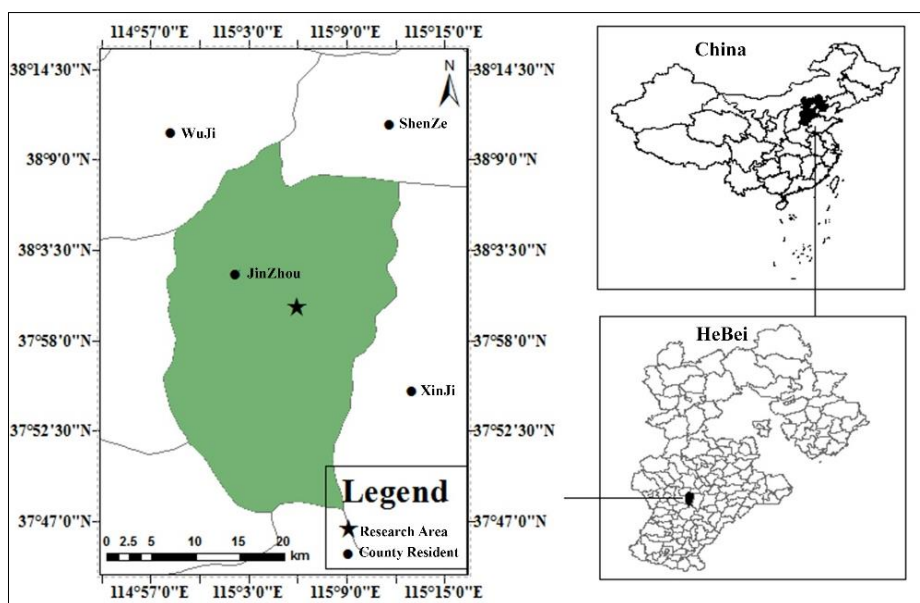
510

511

512

513

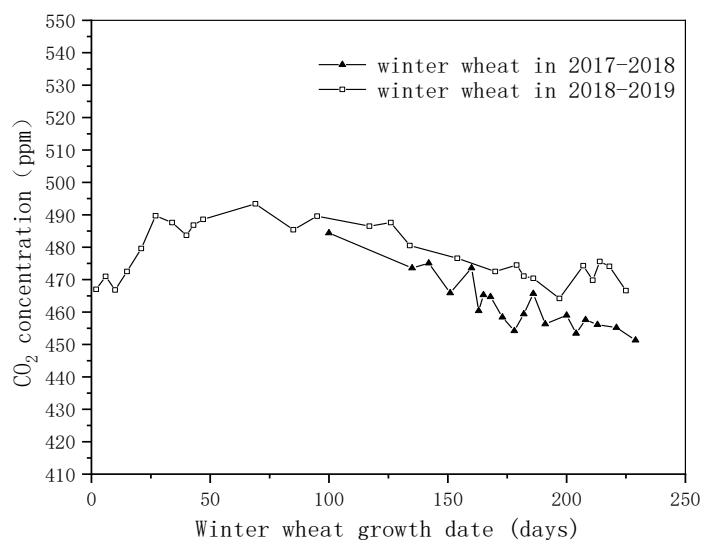
514



515

516

Fig.1 The location of study area



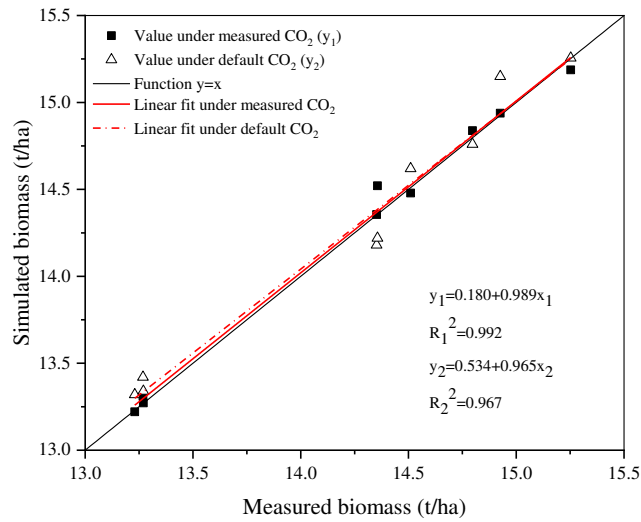
517

518

Fig.2 Variation curve of atmospheric CO₂ concentration in 2017-2019

519

520

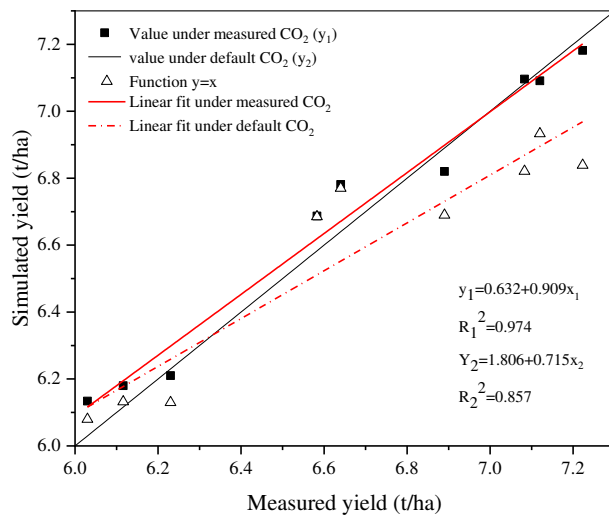


521

522

Figure 3. Linear fitted relationship between measured and simulated values of biomass

523



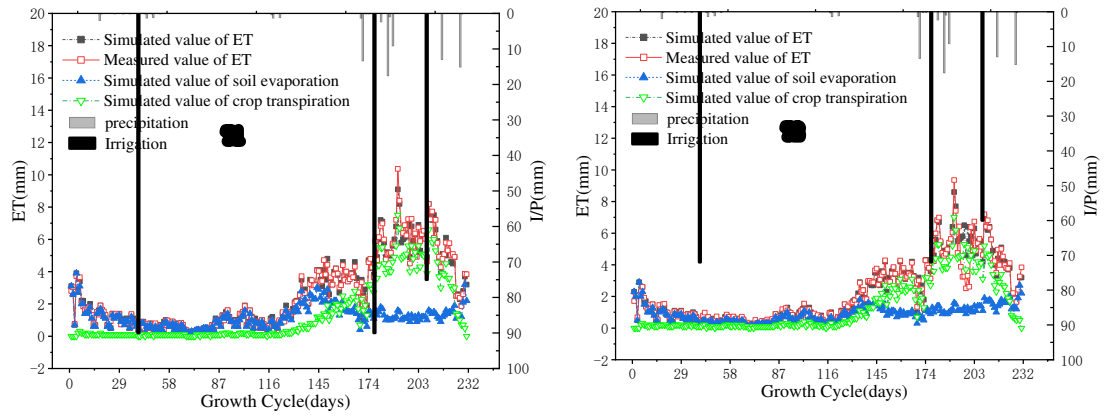
524

525

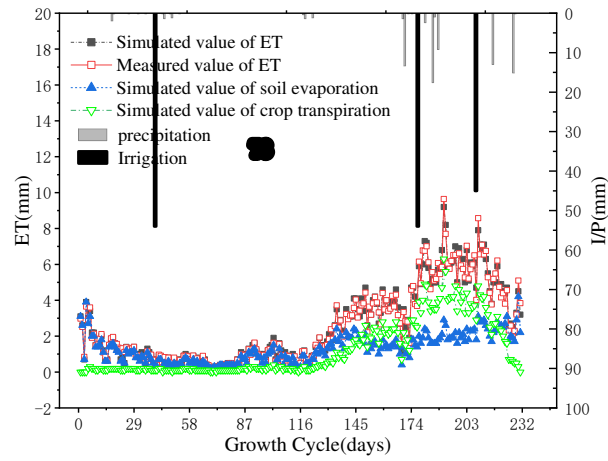
Figure 4. Linear fitting relationship between measured and simulated values of yield

526

527



528



529

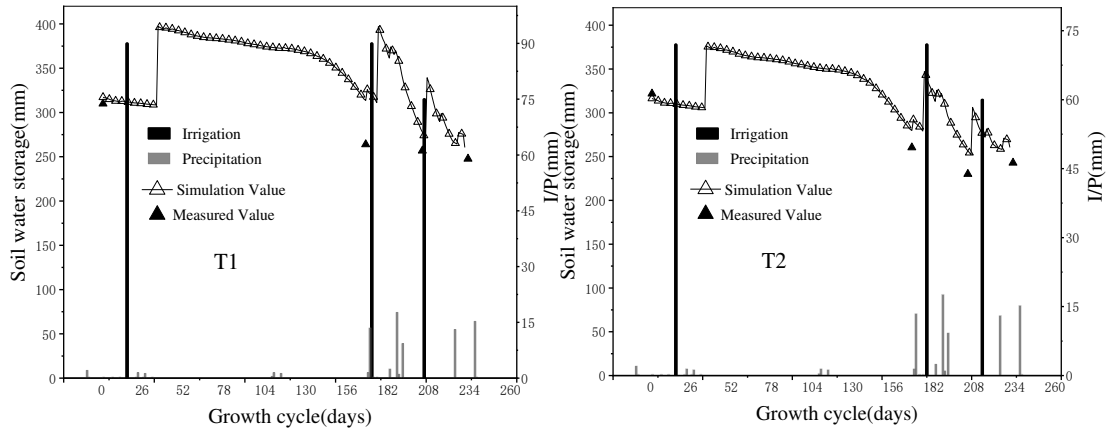
530

Figure 5. The process of field evapotranspiration under different irrigation levels

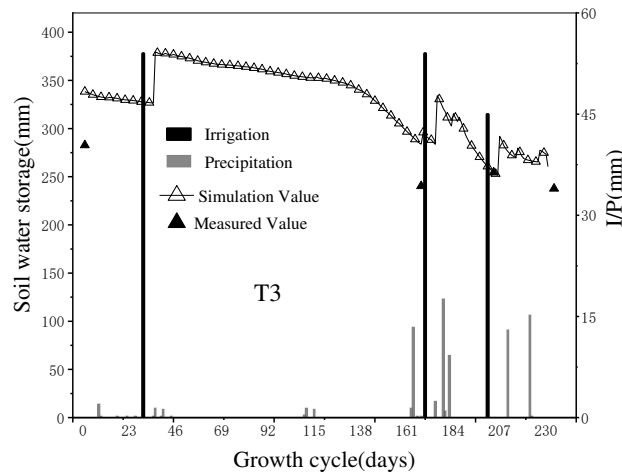
531

532

533



534



535

536 Figure 6. Curves of soil moisture content change under different experimental treatments

537

538

539

Table 1. 2017-2019 winter wheat irrigation scheme

Irrigation date	Net irrigation amount (mm)						
	2017-2018			Irrigation date	2018-2019		
	T1	T2	T3		T1	T2	T3
12.11 (10.25)	60	50	40	11.27 (10.23)	90	72	54
4.2	60	50	40	4.16	90	72	54
5.13	60	50	40	5.17	75	60	45

540

541

542

543

544

Table 2. Soil parameters of study area

Soil parameters	Thickness (cm)					
	0-20	20-40	40-60	60-80	80-100	100-120
Silt content/%	92.04	88.37	90.66	60.32	58.60	57.36
Clay content/%	3.30	4.73	4.46	30.88	31.45	31.88
Sand content/%	4.65	6.90	4.88	8.80	9.95	10.76
Permanent wilting point/m ³ ·m ⁻³	10.6	10.8	11.3	13.6	13.6	14.3
Soil bulk density /g·cm ⁻³	1.21	1.23	1.29	1.38	1.47	1.45
Water content at saturation (weight) /%	42.14	42.63	42.56	46.05	47.17	47.25
Field capacity (weight) /%	32.79	32.58	32.57	33.02	38.84	38.85

545

Table 3. Conservative parameters of AquaCrop model

Describe	Value	Unit
Soil surface covered by an individual seedling at 90% emergence	1.5	cm ²
Base temperature	0.0	°C
Upper temperature	26.0	°C
Crop determinacy linked with flowering	YES	-
Effect of canopy cover in reducing soil evaporation in late season stage	1.5	-
Effect of canopy cover in reducing soil evaporation in late season stage	50	-
Allowable maximum increase (%) of specified HI	15	%
Minimum air temperature below which pollination starts to fail (cold stress)	5	°C
Maximum air temperature above which pollination starts to fail (heat stress)	35	°C
Water productivity normalized for ET ₀ and CO ₂	15.0	g·m ⁻²

546

547

Table 4. Biomass of winter wheat at different irrigation levels (Maunaloa.CO₂)

Planting season	Irrigation level	Biomass (mean)				
		Simulated (t·ha ⁻¹)	Measured (t·ha ⁻¹)	CRM (%)	RMSE(t·ha ⁻¹)	NRMSE (%)
2017-2018	T1	13.372	13.214	-1.193	0.257	1.948
	T2	12.790	13.030	1.844	0.216	1.654
	T3	12.259	12.390	1.063	0.037	0.298
2018-2019	T1	15.028	15.028	-0.004	0.130	0.864
	T2	14.284	14.418	0.932	0.299	2.076
	T3	13.357	13.268	-0.676	0.130	0.981

548

549

550

Table 5. Yield of winter wheat at different irrigation levels (Maunaloa,CO₂)

Planting season	Irrigation level	Grain yield (mean)				
		Simulated (t·ha ⁻¹)	Measured (t·ha ⁻¹)	CRM (%)	RMSE(t·ha ⁻¹)	NRMSE (%)
2017-2018	T1	6.126	6.119	-0.104	0.142	2.327
	T2	5.974	5.970	-0.073	0.037	0.628
	T3	5.641	5.610	-0.559	0.025	0.447
2018-2019	T1	6.921	7.139	3.049	0.238	3.327
	T2	6.733	6.729	-0.059	0.182	2.699
	T3	6.087	6.106	0.311	0.045	0.741

551

552

Table 6. Biomass of winter wheat at different irrigation levels (measured CO₂)

Planting season	Irrigation level	Biomass (mean)				
		Simulated (t·ha ⁻¹)	Measured (t·ha ⁻¹)	CRM (%)	RMSE(t·ha ⁻¹)	NRMSE (%)
2017-2018	T1	13.310	13.214	-0.727	0.204	1.544
	T2	12.968	13.030	0.478	0.099	0.761
	T3	12.248	12.390	1.151	0.057	0.456
2018-2019	T1	15.013	15.028	0.100	0.093	0.616
	T2	14.458	14.418	-0.273	0.114	0.793
	T3	13.270	13.268	-0.020	0.011	0.084

553

554

555

Table 7. Winter wheat yield at different irrigation levels (measured CO₂)

Planting season	Irrigation level	Grain yield (mean)				
		Simulated (t·ha ⁻¹)	Measured (t·ha ⁻¹)	CRM (%)	RMSE(t·ha ⁻¹)	NRMSE (%)
2017-2018	T1	6.193	6.119	-1.204	0.078	1.276
	T2	5.988	5.970	-0.307	0.050	0.843
	T3	5.639	5.610	-0.523	0.073	1.304
2018-2019	T1	7.113	7.139	0.369	0.048	0.679
	T2	6.800	6.729	-1.055	0.130	1.932
	T3	6.153	6.106	-0.759	0.064	1.049

556

557

558

Table 8. Calibration of some parameters of AquaCrop model under two CO₂ databases

Model parameters	Default CO ₂	Measured CO ₂
Planting to maturity(days)	230	230
Maximum rooting depth (m)	1.40	1.40
Harvest index (%)	46	46
Plant density (plants · m ⁻²)	318.75	318.75
Water productivity normalized for ET ₀ and CO ₂ (g·m ⁻²)	15 (15.9)	15 (17.2)
Length building up HI (days)	34	34
Planting to flowering(days)	191	191
Planting to maximum canopy cover(days)	196	196
Maximum canopy cover (%)	96	96
Base temperature (°C)	0	0
Upper temperature (°C)	26	26

559